A Deep Neural Network with Electronic Nose for Water Stress Prediction in Khasi Mandarin Orange Plants

Chayanika Sharma[1,*], **Nairit Barkataki**[1], **Utpal Sarma**[1]

[1]Department of Instrumentation & USIC, Gauhati University, Guwahati-781014, Assam, India

E-mail: chayanika114@gmail.com

February 2023

Abstract. Water stress is a significant environmental factor that hampers plant productivity and leads to various physiological and biological changes in plants. These include modifications in stomatal conductance and distribution, alteration of leaf water potential & turgor loss, altered chlorophyll content, and reduced cell expansion and growth. Additionally, water stress induces changes in the emission of volatile organic compounds (VOCs) across different parts of the plants. This study presents the development of an electronic nose (E-nose) system integrated with a Deep Neural Network (DNN) to detect the presence and levels of water stress induced in Khasi Mandarin Orange plants. The proposed approach offers an alternative to conventional analytical methods that demand expensive and complex laboratory facilities. The investigation employs the leaf relative water content (RWC) estimation, a conventional technique, to evaluate water stress induction in the leaves of 20 plants collected over a span of 9 days after stopping irrigation. Supervised pattern recognition algorithms are trained using the results of RWC measurement, categorising leaves into non-stressed or one of four stress levels based on their water content. The dataset used for training and optimising the DNN model consists of 27,940 samples. The performance of the DNN model is compared to traditional machine learning (ML) methods, including linear and radial basis function Support Vector Machines (SVM), k-Nearest Neighbors (KNN), Decision Tree (DT), and Random Forest (RF). From the results, it is seen that the optimised DNN model achieves the highest accuracy of 97.59% in comparison to other methods. Furthermore, the model is validated on an unseen dataset, exhibiting an accuracy of 97.32%. The proposed model holds the potential to enhance agricultural practices by enabling the detection and classification of water stress in crops, thereby aiding in water management improvements and increased productivity.

Keywords: E-Nose, DNN, Water Stress, Khasi Mandarin Orange

1. Introduction

Agriculture is a crucial sector that supports a considerable portion of the population by producing both food and raw materials for human consumption and industry. But in the near future, agriculture is anticipated to encounter a serious threat due to climate change. Global warming will lead to anomalies in temperature and precipitation, causing a negative impact on agriculture, mostly in underdeveloped countries [1]. Irregularities in rainfall can decrease crop yields and reduce agricultural productivity [2]. Droughts are expected to become more severe because of climate change, leading to a decrease in agricultural productivity. As a result, drought-affected areas are estimated to increase from 15.4% to 44% by 2100 [3]. Drought is defined as the lack of sufficient water availability due to insufficient rainfall over a prolonged period. Droughts happen when the amount of water in the soil is decreased and atmospheric conditions result in a continuous loss of water through transpiration or evaporation [4]. Drought can affect many biochemical and physiological processes in plants such as ABA (abscisic acid) signalling, ion transport, and transcription factors (TFs) activities [5], affecting crop growth and the soil's ability to retain moisture [5].

In addition to that, plants emit a wide range of volatile organic compounds (VOCs) from different parts, such as leaves, flowers, roots, etc. Plants generate these VOCs through various physiological processes and within their different tissues. Changes in VOC emission serve as an involuntary response of plants to alleviate the effects of stress. In 1995, R. C. Ebel, J. P. Mattheis, and D. A. Buchanan discovered that, like other types of stresses, water stress significantly alters the VOC profile of plants [6].

Water stress detection methods need to be optimised at various growth stages of plants. Conventional techniques for assessing plant stress predominantly rely on in-situ methods, which involve measuring variables such as soil moisture and meteorological conditions. These measurements are used to calculate the decrease in moisture within the plant-soil system over a specific time period. S. O. Ihuoma et al. in 2017 [7] discussed different methods for diagnosing water stress in plants. These methods include the gravimetric method, utilisation of soil moisture sensors, soil water balance calculations, measurement of stomatal conductance, estimation of leaf water potential and content, as well as remote sensing methods. Another method, known as crop reflectance monitoring, reported by N. Katsoulas et al. in 2016 [8] involves measuring the variations in plant's reflectance, and this information was utilised to identify the conditions that subject plants to stress. Several other methods were also adopted by researchers to detect the water stress status in different plants, including thermography for canopy temperature measurement [9], the use of a pressure chamber [10], estimation of leaf chlorophyll fluorescence [11], and monitoring the VOC profile [12].

In recent years, the use of an E-nose system for VOC detection has gained considerable attention among the various available methods. This method offers several advantages, including rapid response times, cost-effectiveness, minimal sample preparation, and procedures. Furthermore, one of the notable advantages of using an E-nose system is that it eliminates the requirement for highly skilled professionals to conduct the experiments [12]. An E-nose system collects the VOCs emitted by the leaves of the plants, recognises the gas mixture, and outputs results in the form of fingerprints that represent the unique odor profile of that particular plant. Table 1 describes the difficulties encountered when utilising various methods for detecting water stress in plants.

An E-nose system consists of several key components, including a chemical sensing unit, readout interface circuits, and a soft computing unit for gas recognition. The chemical sensing unit is composed of an array of gas sensors that can detect and respond to different odors with varying sensitivity [13]. The readout interface circuit within the E-nose system converts the sensor outputs into usable electrical signals and stores the data for further analysis [14]. The output of the interface circuit will then be fed to the soft computing unit, which will use various pattern recognition algorithms to provide the final recognition result.

Noise from the E-nose signals can be removed using signal processing techniques such as Principal Component Analysis (PCA), Linear Discriminant Analysis (LDA), Quadratic Discriminant Analysis (QDA), mother wavelet, etc. The methods employed for signal processing aim to determine the optimal

parameters that accurately identify the properties of each signal [15]. In order to overcome the noise contamination of the E-nose signals when monitoring beef quality, the discrete wavelet transform and long short-term memory (DWTLSTM) signal processing technique was proposed by D. R. Wijaya et al. in 2021 [16] and obtained a performance of 94.83% accuracy. A multivariate analysis of variance (MANOVA) test like Wilks' lambda (Λ)-statistics can also be performed to reduce the unwanted noise from the E-nose signals [17]. Other signal processing methods, such as Mahalanobis distance and genetic algorithm, as well as LDA, PCA, and Wilks' lambda statistics, were described by H. Sun et al. in 2017 [18] to reduce the dimension of an E-nose system's output. The reduced dataset must then be fed into machine-learning (ML) methods to produce the recognition result.

Traditional ML algorithms like SVM, KNN, DT, RF, etc. have been adopted by several researchers [19]. These techniques and their combinations are extensively used since they are simple to integrate into the system. Fanglin Mu et al. in 2020 [20] reported a work where the features of the output of an E-nose system were first analysed by signal processing techniques like (LDA), and (PCA) for dimension reduction, and later the ML methods were utilised to obtain the classification model. The best performance was obtained with an accuracy of 95% using the LDA-SVM model to identify the milk source (dairy farm). Similar work has been reported by Xiuguo Zou et al in 2022 [21] for apple quality grading, and used combinations of ML models such as PCA–KNN-SVM (96.45% accuracy) and LDA–KNN-SVM (97.78% accuracy) to improve the accuracy of the learning. The bootstrap ensemble K-Nearest Neighbors (KNN) based prediction model was reported in authors' previous work [22] to obtain better predictive results after using signal processing methods like radial plotting and Wilks' Λ-statistics and achieved maximum accuracy of 99.54%.

ML techniques, however, are not well suited for recognising multiple odours because their anti-noise ability is low, and as discussed earlier, to provide a significant recognition rate the dataset must be passed through several stages. Furthermore, these traditional pattern recognition methods are proven to provide better accuracy when the sample size is small and the number of gas sensors is limited [23, 24]. With the improvement of AI (artificial intelligence) over the past few years, Artificial Neural Network (ANN)-based pattern recognition circuits have been shown to be more successful with flexible topologies [25, 26].

In this study, the authors aim to develop a DNN model specifically designed for a custom-developed E-nose to predict various classes of water stress applied to Khasi Mandarin Orange plants. The performance of the DNN model is compared with several traditional machine learning methods commonly used for classification tasks. These methods include linear and radial basis function Support Vector Machines, KNN, DT, and Rf classifiers. By comparing the performance of the DNN model with these established techniques, the authors aim to assess its effectiveness in predicting and classifying different levels of water stress accurately. To validate the induction of stress in the plants throughout the study, the RWCs of the leaves are simultaneously measured. By measuring RWC in five distinct levels of water-stressed plants, the authors are able to establish a reliable and standardised framework for measuring water stress in the experimental setup.

2. Methodology

A portable and low-cost E-nose system is developed and used to assess water stress in Khasi Mandarin Orange plants. Detailed experimental procedures for the creation of the prototype and analysis of the samples are provided in the subsequent sections of the paper.

2.1. Prototype Development

In Figure 1, the block diagram of the prototype E-nose system is shown. The different parts of the developed prototype are described below.

Table 1. Comparisons of different water stress detection methods

Sl. No.	Authors	Technique used	Challenges
1	Max Gerhards et al (2019) [27]	Thermal infrared (TIR)	Missing temperature thresholds for irrigation scheduling, limited understanding of spectral emissivity and environmental stress on leaf traits, absence of suitable TIR satellite missions, and lack of appropriate data processing methods for TIR remote sensing.
2	Zhuoya Ni et al (2015) [28]	Leaf-level measurements of chlorophyll fluorescence and temperature data	Requirement of costly laboratory equipment & expert operator, high sample preparation time
3	M. P. González et al (2006) [29]	Crop water stress index (CWSI) measurement	The effectiveness of using CWSI to measure water stress depends on the level of crop stress, as it is reliable for low stress, moderately sensitive for moderate stress, but not recommended for highly stressed crops
4	J. M. Fernández et al (2016) [30]	Satellite-based soil moisture measurement	Cost of the sensors & requirement of expert operator

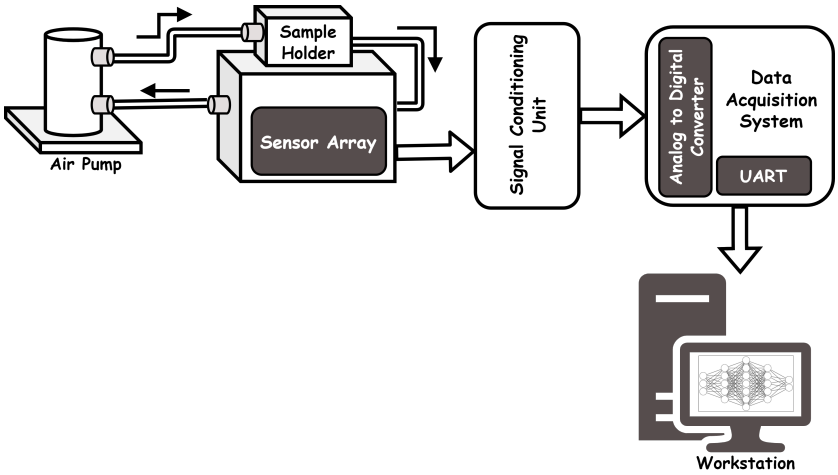

Figure 1. The block diagram of the system

2.1.1. The Gas Sensor Array: In the E-nose prototype, twelve gas sensors are used (shown in Figure 2) to detect the changes in the surrounding airflow. Prior to recording the experimental data, the reference or base resistance values for each gas sensor are determined by introducing fresh air into the sensing chamber. When the leaf-emitted VOCs enter the sensing chamber along with the analysed air, the sensors react to them by altering their output resistance values. The specifics of the sensors used to fabricate the gas sensor array are given in Table 2.

2.1.2. Sample Holder: In the prototype, the sample holding chamber is positioned above the sensor chamber (as shown in Figure 1). An air pump is used to circulate the air, which contains the VOCs emitted from the sample held in the sample holder, between the two chambers.

Table 2. Information of the gas sensors used

Name of the sensors	Target gases	Name of the sensors	Target gases
TGS 2602	NH_3, HS, C_7H_8, and C_2H_5OH	MQ6	LPG, C_4H_{10}, and C_3H_8
TGS 2610	CH_3CH_2OH, H_2, CH_4, $HC(CH_3)_3$, and C_3H_8	TGS 2603	Odor and air contaminants
TGS 2611	CH_4	MQ5	Extremely sensitive to LPG, natural gas, and town gas. Small sensitivity towards smoke and alcohol
TGS 822	CH_4, C_4H_{10}, C_6H_{14}, C_6H_6, C_2H_5OH, CO, and C_3H_6O	MQ3	High sensitivity for alcohols & less sensitive to C_6H_6
TGS 2620	CH_4, CO, C_4H_{10}, H_2, and C_2H_5OH	MQ2	LPG, C_4H_{10}, C_3H_8, CH_4, alcohol, H_2, and smoke
TGS 2600	Sensitive towards gaseous air contaminants	MQ4	Extremely sensitive to CH_4 and natural gas, with only a minor sensitivity to alcohol and smoke

2.1.3. Signal Conditioning Circuit: The signal conditioning circuit shown in Figure 2 generates an equivalent voltage output by converting the resistance change at the gas-sensitive surface of the sensors into a voltage signal. This conversion is achieved through the implementation of a potential divider circuit arrangement within the signal conditioning unit of the developed prototype.

2.1.4. Data Acquisition Unit: The Data Acquisition System (DAQ) utilises an 8-bit Atmel ATmega2560 microcontroller and a 16-channel 10-bit Analog to Digital Converter (ADC), which can handle input voltages from 0V to 5V (as shown in Figure 2). The outputs of the signal conditioning unit are sent to the ADC. The microcontroller collects these digitised signals at a rate of 12 samples per second. Eventually, the ADC outputs are sent to a personal computer via a USB host interface for storage and analysis with data analysis algorithms.

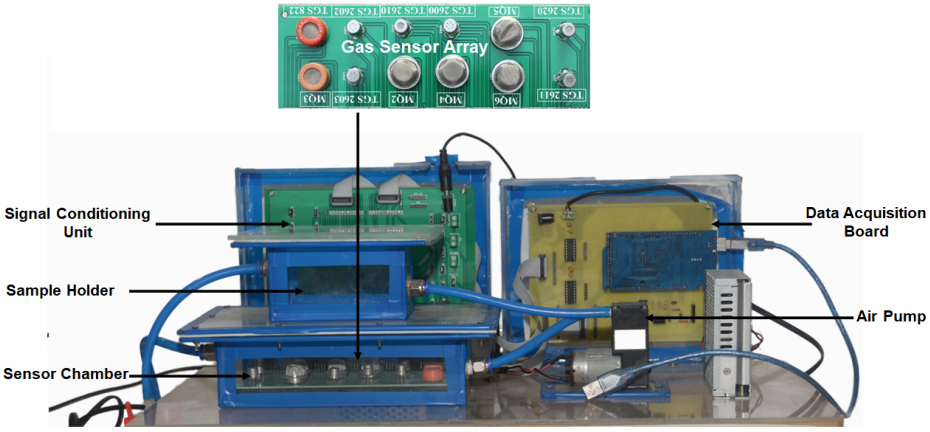

Figure 2. Diagram of the E-nose prototype

2.2. Experimental Sample Preparation

Twenty Khasi Mandarin Orange plants grown in pots (with a top diameter of 30 cm, base diameter of 20 cm, and 28 cm height) are used in the experiments. The physical parameters like temperature, humidity, and light exposure are kept constant for two weeks before starting the experiments. Plants are provided

with 162.85ml/day of water during this period. In order to estimate this value of optimum water supply, factors such as crop evapotranspiration, ET_c ($[mm\ day^{-1}]$) and reference evapotranspiration, ET_0 ($[mm\ day^{-1}]$) must be calculated. The equations to calculate these factors are shown below (the detailed calculations were reported in the author's previous work [31]).

$$ET_0 = \frac{0.408\triangle(Rs - G_f) + \gamma\frac{900}{T+273}V_s(e_p - e_a)}{\triangle + \gamma(1 + 0.34V_s)} \quad (1)$$

$$ET_c = KET_0 \quad (2)$$

where, the parameters R_s, G_f, γ, T, V_s, e_p, e_a, $\triangle$, K describes net radiation of the surface of the crop, heat flux density, psychrometric constant, mean temperature calculated daily at 2m height, speed of wind at a height of 2m, saturation vapour pressure, vapour pressure actual, slope of the vapour pressure curve, and crop coefficient, respectively.

After two weeks of observation, the irrigation to the target plants is halted. The leaf samples are excised on the 1st, 3rd, 5th, 7th, and 9th day after stopping the irrigation to perform the measurements.

2.3. Physiological Measurements

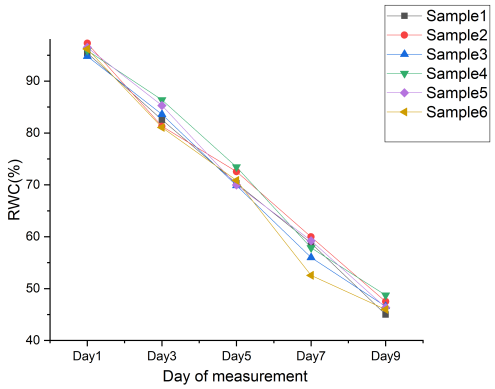

Figure 3. The value of RWC calculated on the day of measurements

The RWC measurements of excised leaves are performed to justify the water stress induction in the sample plants. On each day of measurement, six leaves are kept for RWC measurement. The following equation is used to calculate the RWC of the leaves.

$$RWC = \frac{(W_F - W_D)}{(W_T - W_D)}X100 \quad (3)$$

where, W_F, W_D, and W_T are fresh mass, dry mass, and turgid mass of the excised leaf samples, respectively [32]. In Figure 3, the values obtained after RWC calculation are provided. From this figure, it can be inferred that the leaf RWC values show a negative trend after stopping the irrigation of the sample plants.

3. Data Collection and Analysis

3.1. Collection of Experimental Data

Before taking the measurements, the excised leaf samples are placed in the prototype's sample holding chamber.

3 g of excised Khasi Mandarin Orange leaves are included in each sample set. The signatures of the VOCs are recorded for 240 seconds using twelve gas sensors that comprised the sensor array. A few samples had to be discarded due to null readings in some instances. A total of 27940 samples are taken on the first, third, fifth, seventh, and ninth days after stopping the irrigation, and the conditions of the plants on each day are labelled as non-stressed, Stress-A, Stress-B, Stress-C, and Stress-D, respectively.

For the sake of a detailed comparative analysis, traditional ML approaches along with deep learning neural networks with various parameters are considered.

3.2. ML Approach

ML algorithms including SVM, KNN, DT, and RF are used for the recognition and classification of the dataset. Prior to classification, the entire dataset is divided into 70:30 train-validation sets.

3.3. Deep Learning Approach

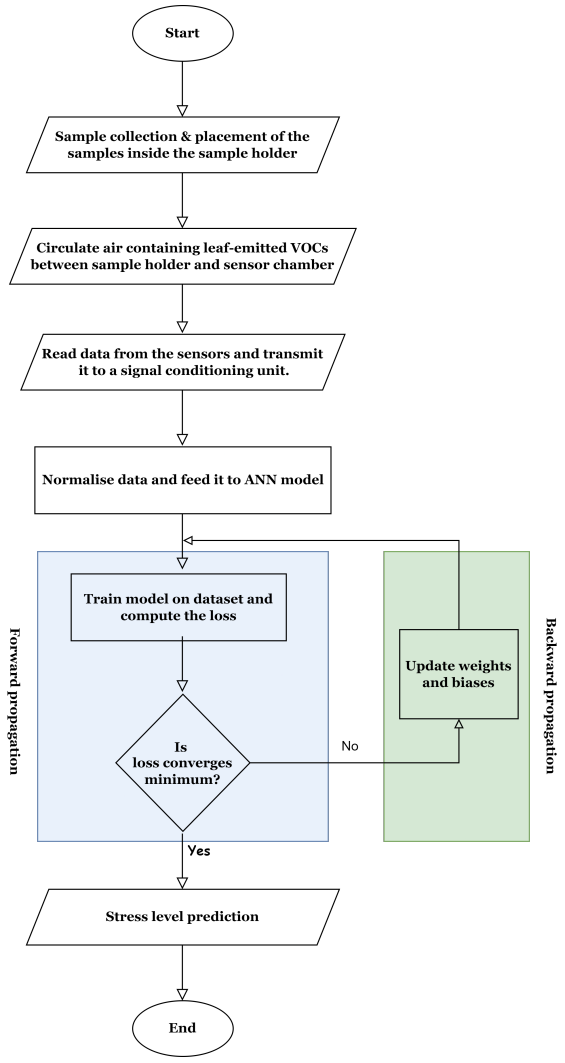

Figure 4. Data collection and analysis protocol

DNN is used in this work to classify plant stress conditions. 19,558 samples (70%) are used for training, and 8382 (30%) are used for validation of the model's performance. The data is normalised, and categorical variables are converted into binary vectors using one-hot encoding. A neural network learns how to classify accurately by minimising errors during the training phase. Each neuron's output is defined by an activation function, and the error is monitored with the help of a loss function. The goal is to reduce the loss to as close to zero as possible. The flowchart for data processing using DNN is shown in Figure 4.

3.3.1. Loss Function: Categorical cross-entropy is used as a loss function during the training of the model. It is used in multi-class classification problems. The goal is to minimise the loss, which means that the smaller the loss, the more efficient the model is.

$$CCE = -\sum_{i=1}^{n} t_i log(p_i) \tag{4}$$

where n is the no. of classes, (P_i) is the softmax probability and (t_i) is the true label for the i^th class. The negative sign helps to ensure that the loss decreases as the distributions approach each other.

3.3.2. Optimisation: Optimisation algorithms minimise the loss function by changing the network's parameters, such as weights and the learning rate. Initially, the model starts training with an initial learning rate value. With successive epochs, the optimiser continuously adjusts the learning rate for the best possible loss. In this work, the model is trained using five optimisers: Adam, Adagrad, Adadelta, Root Mean Squared Propagation (RMSProp), and Adamax, one at a time.

3.3.3. Evaluation Metrics: Accuracy is used as a metric to evaluate the training and validation of the DNN model. It can be used for both binary and multi-class classification problems. Accuracy is defined as the proportion of true outcomes in all instances investigated.

In all, ML algorithms SVC, KNN, DT, and RF, and DNN models with Adam, Adagrad, Adadelta, RMSProp, and Adamax optimisers are used for comparative analysis.

4. Results

The classification results obtained for the SVM classifier with linear and rbf kernels, along with hyperparameter tuning, are shown in Figure 5. To achieve the highest classification accuracy with the SVM classifier, it is necessary to adjust the parameters C and gamma. The C parameter creates a balance between accurately classifying the training samples and maximising the margin of the decision function, while the gamma parameter determines the level of influence a single training sample should have. As shown in the figure, the SVM (linear) classifier demonstrates that gamma had little to no effect on the model's performance, while C=10 achieved the highest accuracy of 73.7%. In the case of the SVM (rbf) classifier, the parameter C is varied from 1 to 1000, and gamma is varied from 0.01 to 0.1. The best accuracy of 96.5% is obtained with C=1000 and gamma=0.1.

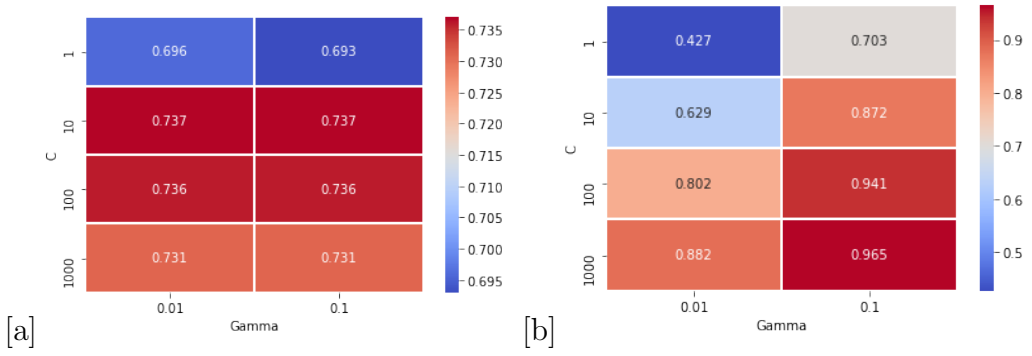

Figure 5. Classification scores with different hyperparameters in SVM classifiers with [a] linear kernel [b] rbf kernel

The KNN classifier's nearest neighbors value is determined to be 6 after multiple training runs, resulting in an accuracy of 94.75%. 'Gini' criterion is used for DT and RF classifiers. The RF classifier's n-estimator value of 100 results in the best accuracy of 93.53%. The classification results obtained using each classifier are given in Table 3.

To train the DNN model, different combinations for the number of neurons in each layer are tested and the number of hidden layers is also adjusted to achieve the best classification accuracy. Even though Adam is one of the best-known optimisers, other popular optimisers are also considered for training the model. Instead of treating the learning rate as a hyperparameter, RMSProp uses an adaptive learning rate. The algorithm divides the learning rate by an exponentially decreasing average of squared gradience and aids in resolving Adagrad's radically decaying learning rate. This is the reason why RMSProp achieves a better validation accuracy of 97.15% compared to Adagrad's 38.24% and Adadelta's 35.51%.

With the Adam algorithm, the accuracy has been achieved at 97.27% compared to other adaptive learning methods. The Adam optimiser is a combination of momentum and the RMSProp optimiser. It combines averages of moving gradients like momentum and utilises the squared gradient to do so like RMSprop to adjust the learning rate parameters. As for Adamax, it is an extension of Adam's gradient descent that generalises the approach to the maxima and may lead to more effective optimisation of some problems. This can be the reason, why it performs slightly better than Adam with a validation accuracy of 97.59% [33, 34]. The higher training accuracy of SVC (rbf) can be attributed to overfitting.

4.1. Final Architecture

The DNN model using Adamax optimiser with an initial learning rate of 0.00001 and three hidden layers had the best validation accuracy of 97.59%. The architecture of this model is shown in Figure 6. The model proposed in this work contains 5 layers along with the input layer. All layers have the ReLU

Table 3. Performance results of different ML and DL techniques in classifying water stress levels in leaves

Sl. No.	Model Used	Training Accuracy	Validation Accuracy
1	SVM (rbf)	98.35%	96.5%
2	SVM (linear)	87.28%	73.7%
3	KNN	97.25%	94.75%
4	DT	97.95%	94.43%
5	RF Classifier	96.86%	93.53%
6	DNN optimizer = Adagrad	39.78%	38.24%
7	DNN optimizer = Adadelta	35.61%	35.51%
8	DNN optimizer = RMSprop	97.35%	97.15%
9	DNN optimizer = Adam	97.43%	97.27%
10	DNN optimizer = Adamax	97.53%	97.59%

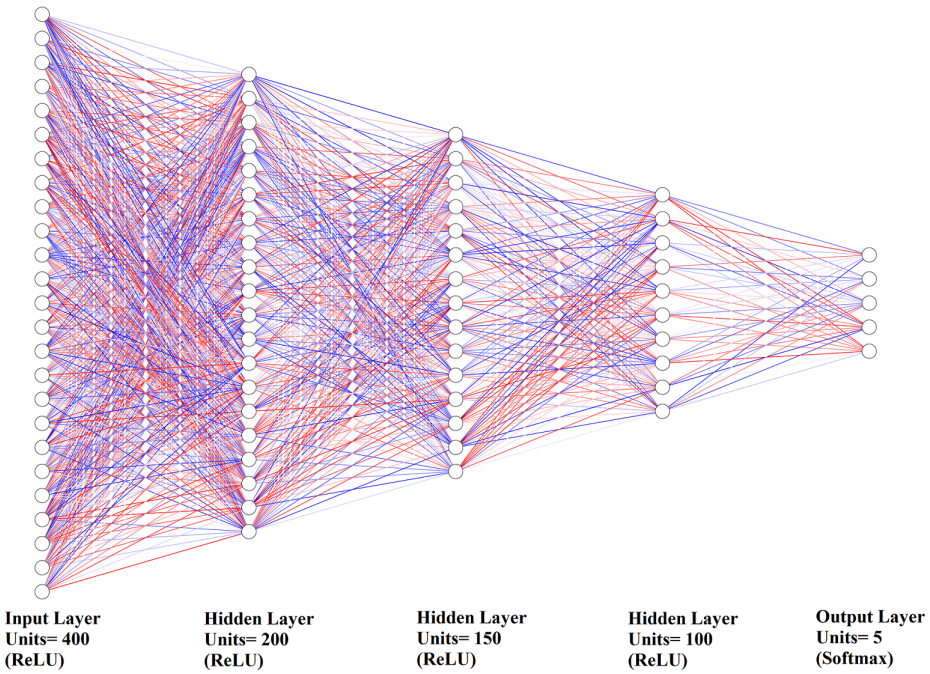

Figure 6. Architecture of the proposed DNN model

(Rectified Linear Unit) activation function. When the input of the neuron is negative, the function outputs 0; otherwise, it returns the same value as the input, as shown in eq. 5.

$$f(n) = max(0, n), \ where \ n \ is \ neuron \ input \tag{5}$$

The input layer consists of 400 units. The number of units is taken as 200, 150, and 100 in the subsequent hidden layers. The number of units in the output layer is taken as 5 to classify the five stress levels and utilises softmax as the activation function.

While training, the validation accuracy is monitored at the end of every epoch of the model. When no further improvement is seen after 50 successive epochs, the training is terminated. In Figure 7, the accuracy at the end of every epoch for each classifier is shown. The total number of epochs varies depending on the optimiser used. For instance, the Adamax optimiser stops training after 930 epochs as no further improvement in accuracy is observed. On the other hand, the models with RMSProp, Adam, Adadelta, and Adagrad optimisers stop training after 445, 597, 357, and 999 epochs, respectively.

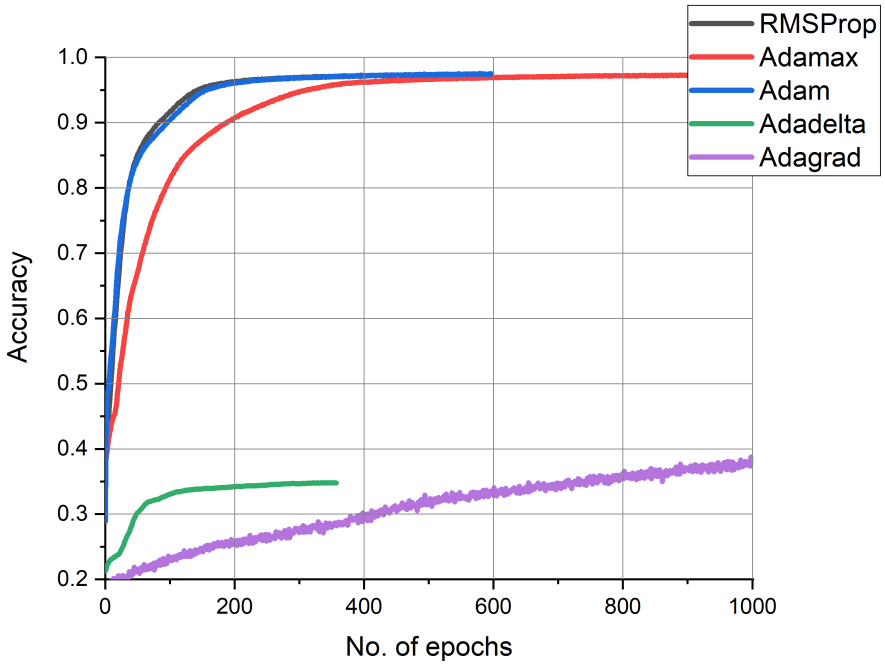

Figure 7. Variation of accuracy during training of the model

As shown in Table 4, various matrices, including F1 score, precision, and recall, are computed to evaluate the model corresponding to five distinct levels of water stress.

Figure 8 depicts the confusion matrix for the model, with the true class labels on the y-axis and the predicted class labels on the x-axis.

Table 4. Classification report of the DNN model on the dataset used for validation

Class	Precision	Recall	F1-score	Overall accuracy
Non-stressed	0.9471	0.9892	0.9677	
Stress-A	0.9973	0.9899	0.9936	
Stress-B	0.9906	0.9958	0.9932	97.59%
Stress-C	0.9580	0.9808	0.9692	
Stress-D	0.9595	0.8749	0.9152	

The capability of a classifier to avoid classifying a negative event as positive is known as precision (P). In Figure 8, the precision in classifying a sample of Stress-C can be calculated as shown in eq. 6. Out of 1334 Stress-C predictions, 1278 are correctly classified as Stress-C.

$$Precision = \frac{1278}{1334} = 0.9580 \tag{6}$$

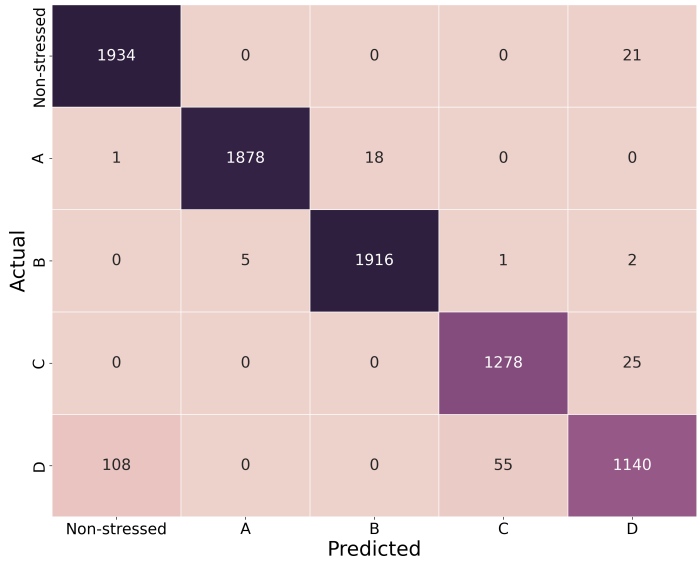

Figure 8. Confusion matrix of the classifier for the validation set

Recall (R) is the ability of the classifier to identify all the positive events. It is calculated as the ratio of true positives to the sum of true positives and false negatives for each class as shown in eq. 7. In the case of Stress-C, out of a total possible 1303, 1278 are correct whereas 25 are false negatives. Recall for Stress-C can therefore be estimated as:

$$Recall = \frac{1278}{1303} = 0.9808 \tag{7}$$

To compare classifier models, F1-score is utilised. It provides the weighted harmonic means of recall and precision, with 1 representing the best result and 0 the worst. Considering the precision and recall for Stress-C, the F1-score can be calculated as shown in eq. 8.

$$F1 = 2 \times \frac{P \times R}{P + R} = 0.9692 \tag{8}$$

4.1.1. Performance of the model on new test data For any instrument or algorithm, repeatability is a primary concern. Therefore, it is important to verify the performance of a DNN model with an unseen or new dataset.

The experimental setup is used to collect 3120 additional data for the final performance evaluation of the proposed model. In Table 5, the classification report of the test dataset is provided. The classification results obtained for random 10 data points out of a total of 3120 data points are shown in Table 6. It basically evaluates the probability of each class. When the model's degree of confidence for a data point is greater than 50% for a specific class, that class is chosen.

Table 5. Classification report of the DNN model on new and unseen experimental dataset

Class	Precision	Recall	F1-score	Overall Accuracy
Non-stressed	0.9531	0.9875	0.9700	
Stress-A	0.9944	0.9875	0.9909	
Stress-B	0.9880	0.9933	0.9906	97.32%
Stress-C	0.9690	0.9864	0.9776	
Stress-D	0.9665	0.9004	0.9323	

Table 6. Prediction with new data

Sl. no	True Class	Probability of the tested sample belonging to					Predicted class
		Non-stressed	Stress-A	Stress-B	Stress-C	Stress-D	
1	Stress-A	1.13E-07	0.579459	0.420412	3.96E-10	0.000129	Stress-A
2	Stress-C	1.51E-14	4.81E-08	0.000162	0.999815	2.30E-05	Stress-C
3	Stress-A	8.12E-12	0.999792	0.000208	9.03E-16	1.45E-11	Stress-A
4	Stress-D	0.00478	4.68E-05	4.80E-07	0.002286	0.992887	Stress-D
5	Stress-D	4.82E-07	9.70E-10	5.54E-05	0.000827	0.999117	Stress-D
6	Stress-C	1.37E-12	2.82E-09	3.28E-05	0.996383	0.003584	Stress-C
7	Stress-C	1.71E-14	3.13E-07	0.001316	0.998675	9.33E-06	Stress-C
8	Stress-D	1.04E-12	1.72E-10	1.36E-05	0.5667648	0.43322164	Stress-C
9	Non-stressed	0.994153	8.66E-05	2.01E-08	2.88E-34	0.00576	Non-stressed
10	Stress-C	3.16E-13	9.10E-11	8.27E-06	0.619269	0.380723	Stress-C

5. Conclusion

This paper describes a detailed comparative analysis to classify water stress levels in Khasi Mandarin plants from a prototype E-nose system. The accuracy of the DNN model using the Adamax optimiser and 3 hidden layers is found to be the highest. The proposed model correctly classified 5 levels of water stress with an accuracy of 97.59%. The performance of the model is further verified on a new and unseen dataset on which its accuracy is 97.32%. However, the classifier does not always classify two adjacent classes with a high degree of confidence. Table 6 shows that the model misclassifies some of the adjacent classes with a very small margin of confidence, as can be seen in serial numbers 1, 8, and 10.

Table 7 shows that previous studies have shown promising results in detecting water stress in plants. The author's previously reported ML classifier [22] was able to detect water stress with an accuracy of 99.54%, but it was unable to distinguish between different levels of stress. In contrast, the works of [36], [37] and [38] proposed deep learning approaches to detect crop water stress from images captured, which showed particularly promising results. However, the performance of their models remains to be tested under different luminosity conditions. The system reported in this work, on the other hand, can take measurements at any time of the day, making it more versatile. This method will enable us to quickly determine the level of induced water stress in Khasi Mandarin plants at any point in time. The model will be particularly useful in the agricultural sector, allowing end-users to detect water stress in plants and verify whether it is due to the shortage of irrigation water or the presence of other factors hindering plant growth. However, in the near future, the same system can be used to collect data on the same set of plants under different environmental conditions. This work may further be extended by developing an automated real-time monitoring system that could alert farmers to water stress in their plants as soon as it is detected.

Table 7. Comparison with past studies of machine learning applications in food and agriculture

Sl. No.	Authors	Technique used	Application	Accuracy
1	Authors' previous work (2022) [22]	E-Nose and bootstrap ensemble K-Nearest Neighbors (KNN) with radial plotting and Wilks' Λ-statistic	E-nose and ML classifier used to detect water stress	99.54%
2	S. S. Virnodkar et al (2020) [35]	Remote sensing and machine learning	For crop water stress determination	83.3% (RF) and 78.3% (XGBoost)
3	M.P. Islam et al (2021) [36]	Deep Neural Network with 417 layers. Pictures of plants collected using smartphone	Detection of water stress in pot-cultivated peach plant	93.00%
4	N. S. Chandel et al (2021) [37]	Deep learning models (Alexnet, GoogLeNet and Inception V3)	Crop water stress detection	The better results were obtained with GoogLeNet (98.3% for maize, 97.5% for okra, and 94.16% for soybean)
5	O. Elsherbiny et al (2022) [38]	A novel hybrid deep network using IoT-based multimodal data	Diagnosing water status in wheat crop	100% with a loss of 0.0012
6	***Present work***	E-nose system allied with a DNN model	Used to detect the presence of water stress and classify it into five levels	97.59% (classification accuracy), 97.32% (Unseen data)

Acknowledgement

The authors acknowledge the Department of Science & Technology, Govt. of India. The authors would like to express gratitude to Mr. Tilak Deka, Glass Blower, Gauhati University, for his constant support during the fabrication of the system. Finally, the authors appreciate the help of Ms. Sharmistha Mazumdar for her input during the preparation of the manuscript from time to time.

Abbreviations:

- DNN- Deep Neural Network
- VOC- Volatile Organic Compound
- MOS- Metal Oxide Semiconductor
- SVM- Support Vector Machines
- KNN- k-Nearest Neighbors
- DT- Decision Tree
- RF- Random Forests
- RWC- Relative Water Content
- PCA- Principal Component Analysis
- LDA- Linear Discriminant Analysis
- QDA- Quadratic Discriminant Analysis
- ADC- Analog to Digital Converter

References

[1] Gurdeep Singh Malhi, Manpreet Kaur, and Prashant Kaushik. Impact of climate change on agriculture and its mitigation strategies: A review. *Sustainability*, 13(3):1318, 2021.

[2] Esha Zaveri, Jason Russ, and Richard Damania. Rainfall anomalies are a significant driver of cropland expansion. *Proceedings of the National Academy of Sciences*, 117(19):10225–10233, 2020.

[3] Yinpeng Li, Wei Ye, Meng Wang, and Xiaodong Yan. Climate change and drought: a risk assessment of crop-yield impacts. *Climate research*, 39(1):31–46, 2009.

[4] Bhaskar Sarma, Neeva Rani Basumatary, Shamsun Nahar, and Bhaben Tanti. Effect of drought stress on morpho-physiological traits in some traditional rice cultivars of kokrajhar district, assam, india. *Ann Plant Sci*, 5(8):1402–1408, 2016.

[5] Yuriko Osakabe, Keishi Osakabe, Kazuo Shinozaki, and Lam-Son P Tran. Response of plants to water stress. *Frontiers in plant science*, 5:86, 2014.

[6] Robert C Ebel, James P Mattheis, and David A Buchanan. Drought stress of apple trees alters leaf emissions of volatile compounds. *Physiologia Plantarum*, 93(4):709–712, 1995.

[7] Samuel O Ihuoma and Chandra A Madramootoo. Recent advances in crop water stress detection. *Computers and Electronics in Agriculture*, 141:267–275, 2017.

[8] Nikolaos Katsoulas, Angeliki Elvanidi, Konstantinos P Ferentinos, Murat Kacira, Thomas Bartzanas, and Constantinos Kittas. Crop reflectance monitoring as a tool for water stress detection in greenhouses: A review. *Biosystems Engineering*, 151:374–398, 2016.

[9] Carlos Ballester, MA Jiménez-Bello, Juan R Castel, and Diego S Intrigliolo. Usefulness of thermography for plant water stress detection in citrus and persimmon trees. *Agricultural and forest Meteorology*, 168:120–129, 2013.

[10] Celia M Rodriguez-Dominguez, Alicia Forner, Sebastia Martorell, Brendan Choat, Rosana Lopez, Jennifer MR Peters, Sebastian Pfautsch, Stefan Mayr, Madeline R Carins-Murphy, Scott AM McAdam, et al. Leaf water potential measurements using the pressure chamber: Synthetic testing of assumptions towards best practices for precision and accuracy. *Plant, Cell & Environment*, 45 (7):2037–2061, 2022.

[11] M Govender, PJ Govender, IM Weiersbye, ETF Witkowski, and F Ahmed. Review of commonly used remote sensing and ground-based technologies to measure plant water stress. *Water Sa*, 35 (5), 2009.

[12] Sudipta Hazarika, Rajdeep Choudhury, Babak Montazer, Subhash Medhi, Manash Protim Goswami, and Utpal Sarma. Detection of citrus tristeza virus in mandarin orange using a custom-developed electronic nose system. *IEEE Transactions on Instrumentation and Measurement*, 69 (11):9010–9018, 2020.

[13] K Arshak, E Moore, GM Lyons, J Harris, and S Clifford. A review of gas sensors employed in electronic nose applications. *Sensor review*, 2004.

[14] Violeta Petrescu, Julia Pettine, Devrez M Karabacak, Marianne Vandecasteele, Mercedes Crego Calama, and Chris Van Hoof. Power-efficient readout circuit for miniaturized electronic nose. In *2012 IEEE International Solid-State Circuits Conference*, pages 318–320. IEEE, 2012.

[15] Mhd Arief Hasan, Riyanarto Sarno, and Shoffi Izza Sabilla. Optimizing machine learning parameters for classifying the sweetness of pineapple aroma using electronic nose. *International Journal of Intelligent Engineering and Systems*, 13(5):122–132, 2020.

[16] Dedy Rahman Wijaya, Riyanarto Sarno, and Enny Zulaika. Dwtlstm for electronic nose signal processing in beef quality monitoring. *Sensors and Actuators B: Chemical*, 326:128931, 2021.

[17] Jin-Young Jeon, Jang-Sik Choi, Joon-Boo Yu, Hae-Ryong Lee, Byoung Kuk Jang, and Hyung-Gi Byun. Sensor array optimization techniques for exhaled breath analysis to discriminate diabetics using an electronic nose. *Etri Journal*, 40(6):802–812, 2018.

[18] Hao Sun, Fengchun Tian, Zhifang Liang, Tong Sun, Bin Yu, Simon X Yang, Qinghua He, Longlong Zhang, and Xiangmin Liu. Sensor array optimization of electronic nose for detection of bacteria in wound infection. *IEEE Transactions on Industrial Electronics*, 64(9):7350–7358, 2017.

[19] Emre Ordukaya and Bekir Karlik. Quality control of olive oils using machine learning and electronic nose. *Journal of Food Quality*, 2017, 2017.

[20] Fanglin Mu, Yu Gu, Jie Zhang, and Lei Zhang. Milk source identification and milk quality estimation using an electronic nose and machine learning techniques. *Sensors*, 20(15), 2020. ISSN 1424-8220. doi: 10.3390/s20154238. URL `https://www.mdpi.com/1424-8220/20/15/4238`.

[21] Xiuguo Zou, Chenyang Wang, Manman Luo, Qiaomu Ren, Yingying Liu, Shikai Zhang, Yungang Bai, Jiawei Meng, Wentian Zhang, and Steven W. Su. Design of electronic nose detection system for apple quality grading based on computational fluid dynamics simulation and k-nearest neighbor support vector machine. *Sensors*, 22(8), 2022. ISSN 1424-8220. doi: 10.3390/s22082997. URL `https://www.mdpi.com/1424-8220/22/8/2997`.

[22] Chayanika Sharma, Rajdeep Choudhury, and Utpal Sarma. Sensor array optimization to design and develop an electronic nose system for the detection of water stress in khasi mandarin orange. *Journal of Circuits, Systems and Computers*, page 2250172, 2022.

[23] Yan Shi, Furong Gong, Mingyang Wang, Jingjing Liu, Yinong Wu, and Hong Men. A deep feature mining method of electronic nose sensor data for identifying beer olfactory information. *Journal of food engineering*, 263:437–445, 2019.

[24] Vera Schroeder, Ethan D Evans, You-Chi Mason Wu, Constantin-Christian A Voll, Benjamin R McDonald, Suchol Savagatrup, and Timothy M Swager. Chemiresistive sensor array and machine learning classification of food. *ACS sensors*, 4(8):2101–2108, 2019.

[25] S Ramesh, C Yaashuwanth, K Prathibanandhi, Adam Raja Basha, and T Jayasankar. An optimized deep neural network based dos attack detection in wireless video sensor network. *Journal of Ambient Intelligence and Humanized Computing*, pages 1–14, 2021.

[26] Aramesh Rezaeian, Marzieh Rezaeian, Seyede Fatemeh Khatami, Fatemeh Khorashadizadeh, and Farshid Pouralizadeh Moghaddam. Prediction of mortality of premature neonates using neural network and logistic regression. *Journal of Ambient Intelligence and Humanized Computing*, pages 1–9, 2022.

[27] Max Gerhards, Martin Schlerf, Kaniska Mallick, and Thomas Udelhoven. Challenges and future perspectives of multi-/hyperspectral thermal infrared remote sensing for crop water-stress detection: A review. *Remote Sensing*, 11(10):1240, 2019.

[28] Zhuoya Ni, Zhigang Liu, Hongyuan Huo, Zhao-Liang Li, Françoise Nerry, Qingshan Wang, and Xiaowen Li. Early water stress detection using leaf-level measurements of chlorophyll fluorescence and temperature data. *Remote Sensing*, 7(3):3232–3249, 2015.

[29] MP González-Dugo, MS Moran, L Mateos, and R Bryant. Canopy temperature variability as an indicator of crop water stress severity. *Irrigation Science*, 24(4):233–240, 2006.

[30] José Martínez-Fernández, A González-Zamora, Nilda Sánchez, A Gumuzzio, and CM Herrero-Jiménez. Satellite soil moisture for agricultural drought monitoring: Assessment of the smos derived soil water deficit index. *Remote Sensing of Environment*, 177:277–286, 2016.

[31] Rajdeep Choudhury, Sudipta Hazarika, and Utpal Sarma. Detection of water stress in khasi mandarin orange plants from volatile organic compound emission profile implementing electronic nose. *Int. J. Eng. Adv. Technol.*, 9(1):133–137, 2019.

[32] Michael R Schlemmer, Dennis D Francis, JF Shanahan, and James S Schepers. Remotely measuring chlorophyll content in corn leaves with differing nitrogen levels and relative water content. *Agronomy journal*, 97(1):106–112, 2005.

[33] Prudhvi Varma. *Understanding Adaptive Optimization techniques in Deep learning*. DEVELOPERS CORNER, Jul 2020. URL `https://analyticsindiamag.com/understanding-adaptive-optimization-techniques-in-deep-learning/`.

[34] Akshay Chandra. *Learning Parameters, Part 5: AdaGrad, RMSProp, and Adam.* Towards Data Science, Sep 2019. URL `https://towardsdatascience.com/learning-parameters-part-5-65a2f3583f7d`.

[35] Shyamal S Virnodkar, Vinod K Pachghare, VC Patil, and Sunil Kumar Jha. Remote sensing and machine learning for crop water stress determination in various crops: a critical review. *Precision Agriculture*, 21(5):1121–1155, 2020.

[36] Md Parvez Islam and Takayoshi Yamane. Hortnet417v1—a deep-learning architecture for the automatic detection of pot-cultivated peach plant water stress. *Sensors*, 21(23):7924, 2021.

[37] Narendra Singh Chandel, Subir Kumar Chakraborty, Yogesh Anand Rajwade, Kumkum Dubey, Mukesh K Tiwari, and Dilip Jat. Identifying crop water stress using deep learning models. *Neural Computing and Applications*, 33:5353–5367, 2021.

[38] Osama Elsherbiny, Lei Zhou, Yong He, and Zhengjun Qiu. A novel hybrid deep network for diagnosing water status in wheat crop using iot-based multimodal data. *Computers and Electronics in Agriculture*, 203:107453, 2022.